Analysis of Tropical Cyclone Eye Slope Using Airborne Radar Reflectivity Data: Composites and a Case Study from Hurricane Earl (2010) using GRIP APR2 data.

Andrew T. Hazelton (ath09c@my.fsu.edu) and Robert E. Hart
Department of Earth, Ocean, and Atmospheric Science, Florida State University, Tallahassee, FL

I. Introduction/Background

The slope of the hurricane eye/eyewall has been documented observationally since at least the 1950s, and the Sawyer-Eliassen model for tropical cyclones explains dynamically why the eyewall should tilt. However, the relationship between slope and intensity has proven to be a difficult research problem. Studies investigating slope and its relationship with intensity have mostly focused on the slope of the radius of maximum wind (RMW), and have produced conflicting results on the correlation between slope and intensity. Shea and Gray (1973) used aircraft wind observations to show a possible relationship between RMW slope and intensity. However, Stern and Nolan (2009) used airborne Doppler Radar velocity data to show that there was little relationship, even for individual storms. In this study, we use a different metric, which is based on a radar reflectivity threshold and attempts to find the actual edge of the eye. We develop a dataset of eye slopes using airborne radar reflectivity data from several different sources. The analysis shown here consists of composite results as well as a case study for Hurricane Earl (2010) using APR-2 radar data from the GRIP campaign.

II. Data and Methodology

For this project, we used data from the NASA Convection and Moisture (CAMEX) field project, the NASA Genesis and Rapid Intensification Project (GRIP), and radar data from the Hurricane Hunter flights into Atlantic and Eastern Pacific Hurricanes. To calculate eye slope, we developed an algorithm that starts at the storm center and then goes out in each direction until it hits a threshold value of reflectivity. The algorithm was only used between heights of 2 km and 10.5 km. The lower boundary was put in place to avoid contamination from boundary-layer processes such as sea spray, and the upper limit was implemented so that there was a standard height between all three data platforms. The height and horizontal distance where this threshold value is reached are then used to calculate the slope, using least-squares linear regression. We then used the inverse of this slope as our slope measurement, to keep upright slopes from becoming excessively large. Figure 1 shows a map of all of the different slope measurements taken (100 in all). Figure 2 is a histogram showing the distribution of inverse slopes.

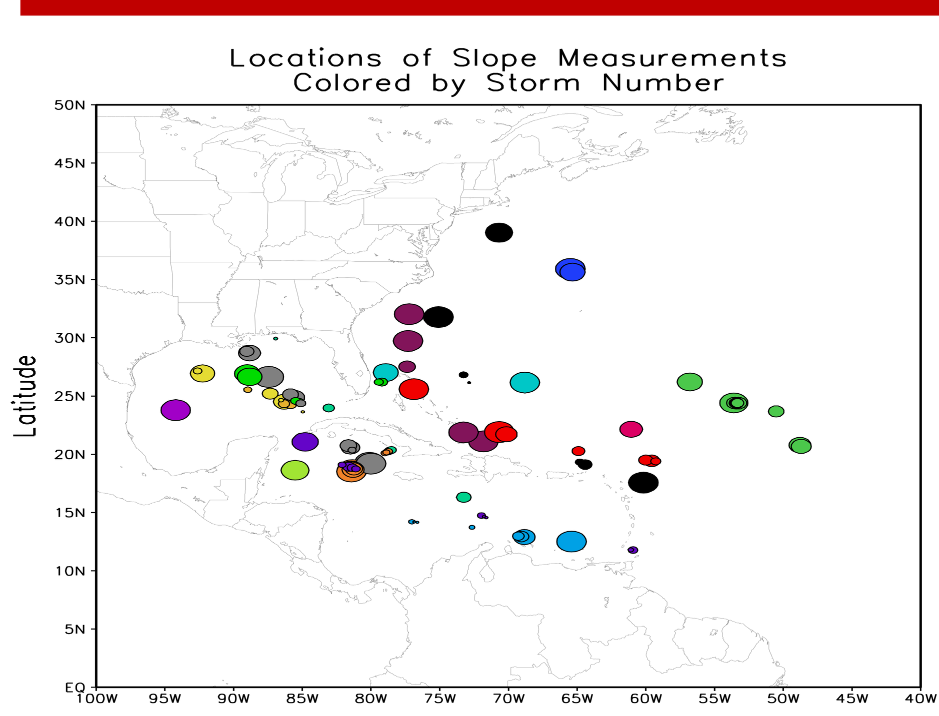

Figure 1: Locations of slope measurements. The colors represent different storms, and the size of the circle is proportional to the (inverse) eye slope. Larger circles correspond to more tilted eyes, and smaller circles represent more upright eyes.

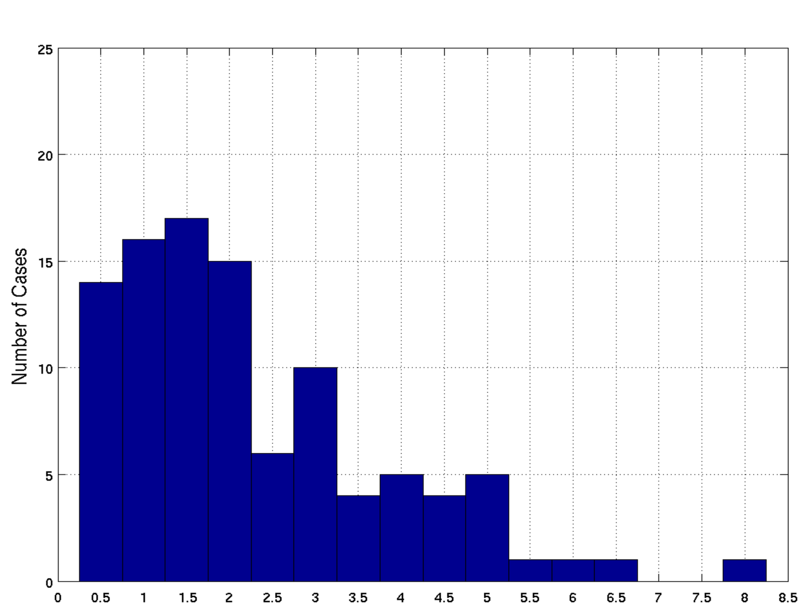

Figure 2: Distribution of inverse slopes for all 100 cases analyzed in this study. Note that 0 represents a perfectly upright eye, 1 represents a 45 degree tilt, and larger numbers denote increasingly tilted eyes. The peak in the distribution is 1-1.5, and the large tail is due to a few cases with very shallow, tilted eyewalls.

III. Composite Results

Figure 3 shows the relationship between eye slope and minimum central pressure based on the vortex messages from Hurricane Hunter flights. The relationship is indeed statistically significant (r = 0.38, p < 0.01). Figure 4 shows the correlations between slope and intensity for most of the storms analyzed in this study. This graph shows that there is significant variability in the slope-intensity relationship from storm to storm, with some storms showing a high correlation and other storms showing little to no relationship. Case studies highlighting Hurricane Felix (a strong relationship case) and Hurricane Ivan (a weak relationship case) are examined in Hazelton and Hart (2012).

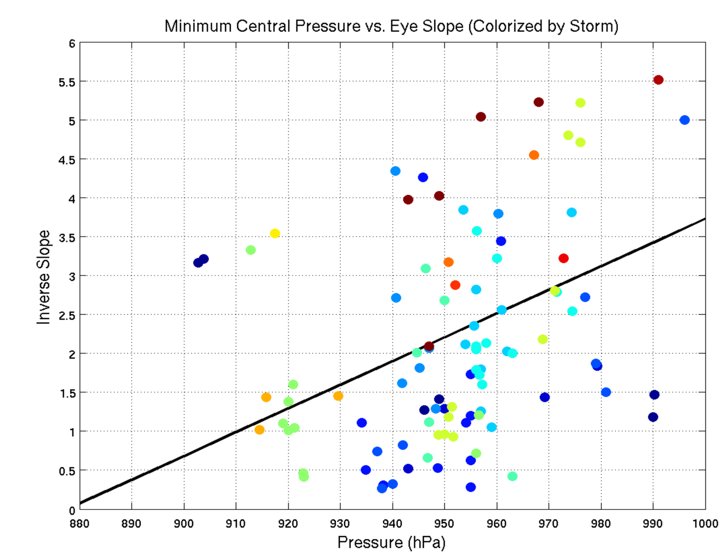

Figure 3: Relationship between eye slope and storm intensity (minimum central pressure). The correlation is statistically significant (r= 0.38, p < 0.01).

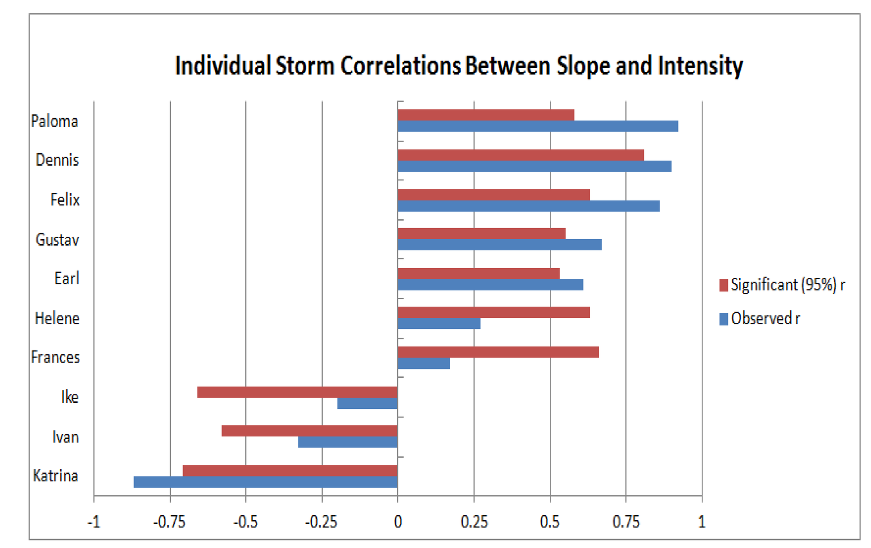

Figure 4: Relationship between eye slope and storm intensity for individual storms. Red bars show the actual correlation, blue bars show the correlation that would be significant at 95% confidence, based on the number of points for each storm.

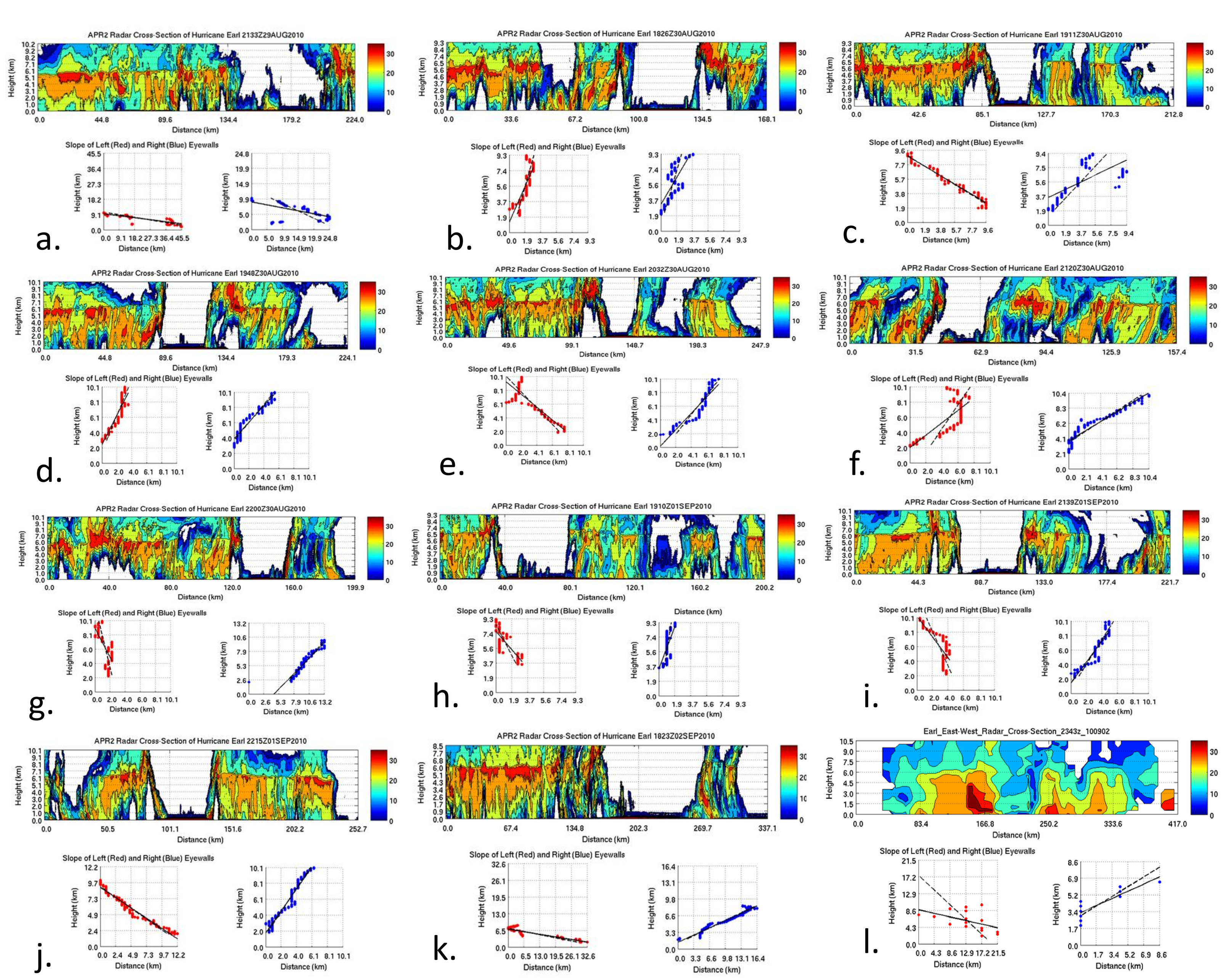

Figure 5: Radar cross-sections through the eye of Hurricane Earl (2010) from 2133 UTC 29 August through 2343 UTC 03 September. Figs. 4a-4k are from the APR2 radar data aboard the NASA DC-8 during GRIP, and Fig. 4l is from the tail radar from the NOAA-P3 flight from the Hurricane Research division. Below each cross-section is the result of the slope calculation for each side of the eye based on the edge-detection algorithm and linear regression.

IV. Case Study: Hurricane Earl (2010)

Hurricane Earl in 2010, which was one of the TCs sampled extensively during GRIP, was one of the cases for which there was a statistically significant relationship between slope and intensity (r = 0.61, p = 0.03). Figure 5 shows a series of radar cross-sections through Earl from August 29 to September 3, and shows how the eye became more upright as the storm strengthened and then became more tilted as the storm weakened later in the period. Figure 6 shows time series of normalized inverse slope and minimum central pressure in Earl, and again shows how the eye became more upright as the storm strengthened and then became less upright prior to and during the weakening phase. It is also interesting to note how three eye crosses on August 30 showed the eyewall tilting inward. All three of these crosses were from North-South, indicating that the eyewall was tilting southward. This tilt was likely caused by Earl interacting with an upper-level trough to the north (Figure 7). The shear associated with the trough probably caused the eyewall to tilt over, and the Sawyer-Eliassen response to the momentum flux from the north seems to have caused enhanced upward motion and convection in the northern eyewall (Molinari and Vollaro 1989). This enhanced convection can be seen in the satellite imagery in Figure 8.

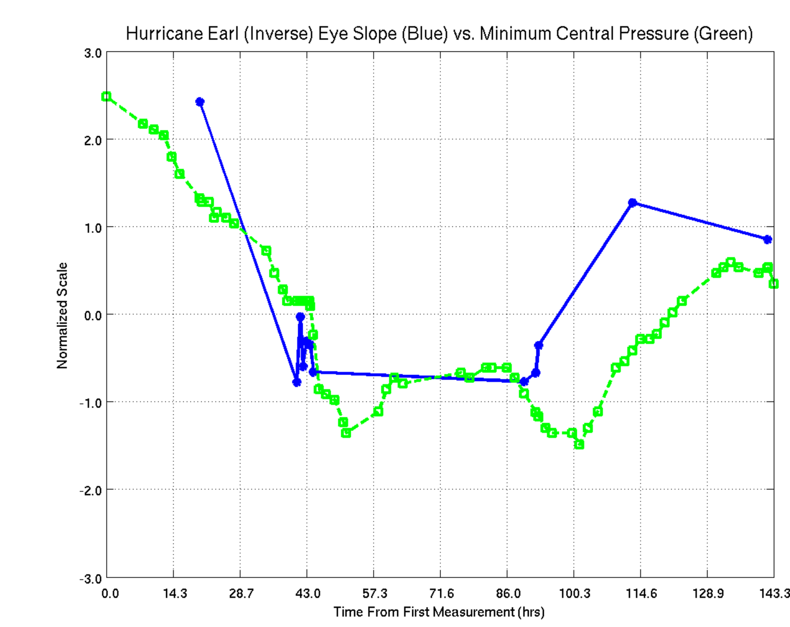

Figure 6: Time series of normalized inverse slope vs. minimum central pressure in Earl. Smaller numbers represent more upright eyes and lower pressure.

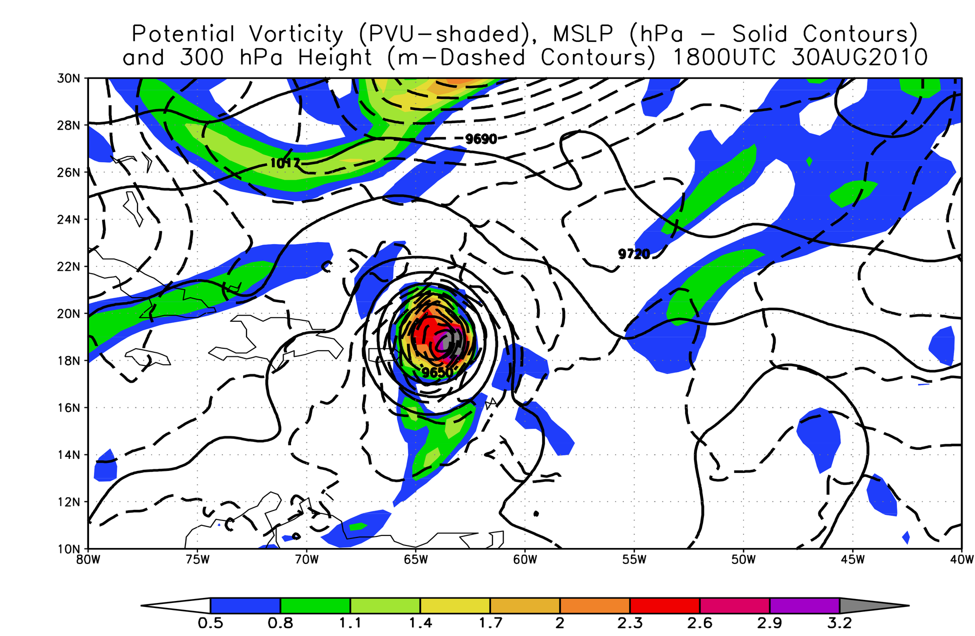

Figure 7: Sea Level Pressure, 300 hPa Height, and 300 hPa potential vorticity at 1800 UTC 30 August 2010, showing Hurricane Earl interacting with the trough to its north and west.

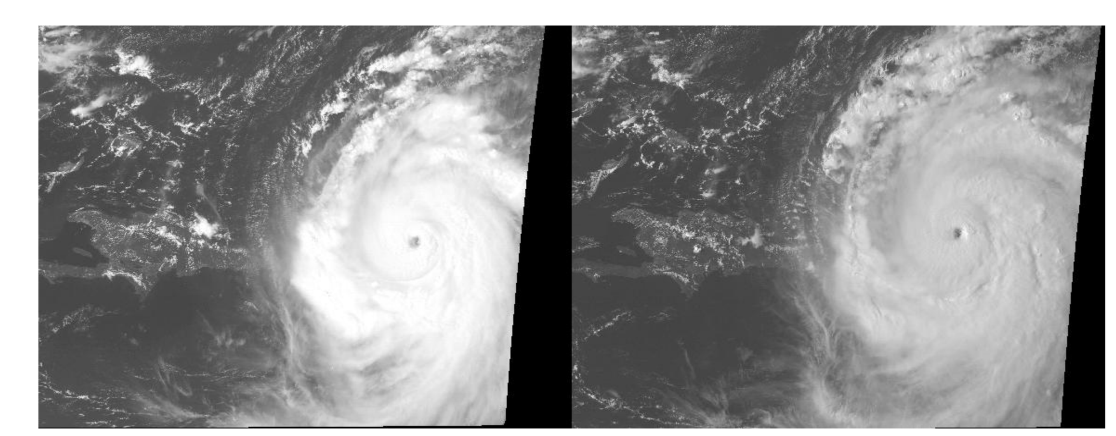

Figure 8: Visible imagery of Hurricane Earl at a) 1825 UTC 30 August and b) 1955 UTC 30 August 30. Note the convective burst in the north and east eyewall in both cases. Image from the NRL Monterey Marine Meteorology Division.

V. Acknowledgements

The authors would like to thank Stephen Durden at NASA JPL for providing information about the APR2 radar data, and Rob Rogers at NOAA HRD for providing details about the HRD radar data. Nick Shay and Jodi Brewster at the University of Miami RSMAS provided OHC data for another case study. Partial support for this work came from an AMS/ITT Graduate Fellowship, the Florida State University Legacy Fellowship, and NASA GRIP Grant #NNX09AC43G.

References:

-Gamache, J.F., 1997: Evaluation of a fully three-dimensional variational Doppler analysis technique. Preprints, *28th Conf. on Radar Meteorology*, Austin, TX, Amer. Meteor. Soc., 422-423.
-Hazelton, A.T. and R.E. Hart, 2012: Analysis of Hurricane Eye Slope Using Reflectivity Data From Airborne Doppler Radar: Composites and Case Studies. Preprints, *30th Conf. on Hurricanes and Tropical Meteorology*, Ponte Vedra Beach, FL, Amer. Meteor. Soc., 4 pp.
-Molinari, J. and D. Vollaro, 1989: External influences on hurricane intensity. Part I: Outflow layer eddy angular momentum fluxes. *J. Atmos. Sci.*, **46**, 1093-1105.
-NRL Monterey Marine Meteorology Division, cited 2012: TC_PAGES Page. [Available online at: http://www.nrlmry.navy.mil/TC.html.]
-Saha, S. and coauthors, 2010: The NCEP Climate Forecast System Reanalysis. *Bull. Amer. Meteor. Soc.*, **91**, 1015–1057.
-Shea, D.J., and W.M. Gray, 1973: The hurricane's inner core region. I. Symmetric and asymmetric structure. *J. Atmos. Sci.*, **30**, 1544-1564.
-Stern, D.P. and D.S. Nolan, 2009: Reexamining the vertical structure of tangential winds in tropical cyclones: observations and theory. *J. Atmos. Sci.*, **66**, 3579-3600.